Fluorescence of methylated derivatives of hydroxyphenylimidazopyridine. Resolution of strongly overlapping spectra and a new ESIPT dye showing very efficient radiationless deactivation

Alfonso Brenlla, Manoel Veiga, M. Carmen Ríos Rodríguez, Manuel Mosquera and Flor Rodríguez-Prieto

Photochem. Photobiol. Sci., 2011, **10**, 1622. DOI: 10.1039/c1pp05165b, which has been published in final form at http://pubs.rsc.org/en/content/articlelanding/2011/pp/c1pp05165b

Fluorescence of methylated derivatives of hydroxyphenylimidazo-pyridine. Resolution of strongly overlapping spectra and a new ESIPT dye showing very efficient radiationless deactivation

Alfonso Brenlla,[a] Manoel Veiga,[a] M. Carmen Ríos Rodríguez,*[a] Manuel Mosquera*[a] and Flor Rodríguez-Prieto*[a]

Received (in XXX, XXX) Xth XXXXXXXXX 200X, Accepted Xth XXXXXXXXX 200X
First published on the web Xth XXXXXXXXX 200X
DOI: 10.1039/b000000x

The ground- and excited-state behaviour of the isomeric species 2-(2'-methoxyphenyl)imidazo [4,5-*b*]pyridine (**1-OMe**) and 2-(2'-hydroxyphenyl)-4-methylimidazo[4,5-*b*]pyridine (**1-NMe**) in neutral and acid media has been studied by UV-vis absorption spectroscopy, steady-state and time-resolved fluorescence spectroscopy. The new dye **1-NMe** is non-fluorescent in neutral media except in trifluoroethanol, where it shows a very weak fluorescence. **1-NMe** exhibits also highly solvent-dependent fluorescence intensity in acidic media. We propose that the neutral species experiences a fast excited-state intramolecular proton transfer (ESIPT), relaxing afterwards by intramolecular twisting associated with internal charge transfer (TICT) and subsequent very fast internal conversion of the proton-transferred TICT structure. The behaviour of **1-NMe** in acidic media is explained by the existence of a ground-state tautomeric equilibrium between species with intramolecular hydrogen bonds N–H···OH and N···H–O. The first type of tautomers dissociates at the hydroxyl group in water and ethanol, but fluoresces in acetonitrile and trifluoroethanol due to the inability of these solvents to accept the proton. The second type of tautomers is non-emissive due to fast radiationless deactivation through an ESIPT-TICT process. The fluorescence of **1-OMe** was investigated in neutral and acidic media, demonstrating the photobasic character of the pyridine nitrogen. A ground-state equilibrium between pyridinium and imidazolium cations was found for this species, showing overlapping absorption and fluorescence spectra. We devised a method to resolve the spectra by applying principal component global analysis to a series of excitation spectra taken at different emission wavelengths, which allowed estimation of the equilibrium constant between the cations.

1. Introduction

Among the various intramolecular processes induced by light absorption, the excited-state intramolecular proton transfer (ESIPT)[1-5] and the intramolecular charge transfer (ICT)[6, 7] lie at the heart of many photochemical and photobiological processes. A special case of ICT processes are those leading to twisted structures (twisted intramolecular charge-transfer states, or TICT states), which are commonly encountered for a wide variety of molecular species.[7, 8] The widespread interest in ESIPT and ICT processes encompass fundamental studies of intramolecular processes[1-10] and applications as sensors in biological and chemical systems[11-15] or as advanced devices for lasing, optical storage and electroluminescence.[16-18]

The interplay between intramolecular proton- and charge-transfer processes is a topic of long-standing research interest,[19-36] related to the more general subject of proton-coupled electron transfer.[6, 37, 38] In this paper, we study a pair of isomeric species (see Fig. 1) that may experience ESIPT and TICT processes.

Many ESIPT and TICT molecules are well known by their

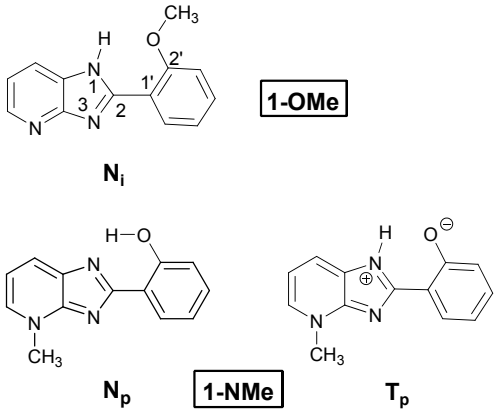

Fig. 1 Molecular structures of the compounds studied in this work, **1–OMe** and **1–NMe**. The normal forms ($\mathbf{N_i}$ and $\mathbf{N_p}$) and the tautomer $\mathbf{T_p}$ obtained for **1–NMe** after ESIPT are shown. Subscript **i** indicates that a H atom is bonded to an imidazole N, whereas subscript **p** designates the structure with a hydrogen or methyl group attached to the pyridine N.

ability to act as very efficient UV absorbers, used for photoprotection in sunscreens and polymer photostabilizers.[28, 39, 40] It has long been known for ESIPT molecules that the photoprotection efficiency depends on an intact intramolecular hydrogen bond, essential for the ultrafast intramolecular proton transfer in the excited state.[40] The phototautomer produced in the ESIPT process undergoes a fast radiationless deactivation which transforms the absorbed radiation energy into innocuous thermal energy, providing the basis for the photoprotective activity.

The involvement of a large-amplitude motion[28-36, 41-52] and an intramolecular charge-transfer process[28-36, 47-49, 51] in the fast radiationless deactivation of several ESIPT phototautomers has been reported by several authors. In favourable cases, the emission of an ICT state was detected.[25-27] We and others proposed that the efficient radiationless deactivation of the proton-transferred phototautomer is often connected with the capacity of this species to form a TICT state, which decays at ultrafast rate.[31-36, 47-49] The efficiency of the TICT process depends, in turn, on the facility to achieve twisted structures[28, 33, 35, 49] and on the strength of the electron donor (deprotonated moiety) and electron acceptor (protonated moiety) of the phototautomer. Electron-withdrawing groups introduced in the protonated moiety, or electron-donating groups introduced in the deprotonated moiety, facilitate therefore the TICT process, with concomitant enhancement of the radiationless deactivation and photoprotector efficiency.[28, 29, 35, 49, 53] On the contrary, electron-withdrawing substituents introduced in the deprotonated moieties of several ESIPT molecules decrease the rate of the radiationless deactivation and increase consequently their fluorescence quantum yields.[53] Various authors have stressed the relevance of this knowledge for the design of new ESIPT dyes useful as UV absorbers or fluorescent probes.[28, 53]

As mentioned above, a key factor that modulates the efficiency of the TICT process of the proton-transferred phototautomer is the strength of the electron donor and electron acceptor. For example, no experimental evidence for TICT deactivation was found for the phototautomer of 2-(2'-hydroxyphenyl)benzimidazole (HBI),[35] but its derivatives bearing a better electron donor (an amino or dialkylamino group at C4') were found to undergo a fast radiationless deactivation, which was interpreted as a coupled ESIPT-TICT process.[49] To further test this model, we investigate in this work the ground- and excited-state behaviour of the HBI derivatives **1-OMe** and **1-NMe** (see Fig. 1). The last species may undergo an ESIPT process, giving rise to the proton-transferred phototautomer $\mathbf{T_p}$ from the normal form $\mathbf{N_p}$. On the contrary, its isomer **1-OMe** is unable to undergo ESIPT, as it lacks the hydroxyl hydrogen, but both **1-OMe** and **1-NMe** could in turn experience a TICT process. Given that the imidazopyridine moiety of these molecules possesses higher electron-acceptor ability than the benzimidazole moiety of HBI, we expect the TICT process to be enhanced for **1-OMe** and **1-NMe**. Quantum-mechanical calculations already predicted an ESIPT-TICT process for related azo derivatives of HBI,[50] and dual emission due to a TICT process was demonstrated for 2-(4'-*N*,*N*-dimethylamino)phenylimidazo [4,5-*b*]pyridine.[54, 55]

In this paper, we elucidate the ground-state equilibria and the excited-state proton- and charge-transfer processes of **1-NMe** and **1-OMe**, in different solvents and acidity conditions. To the best of our knowledge, **1-NMe** is a new species which has not been described before. **1-OMe** was previously prepared and its therapeutic effects demonstrated.[56-58] The photophysical behaviour of **1-OMe** was investigated by Dogra et al. in several solvents at various acidities by means of absorption and fluorescence spectroscopy and semi-empirical quantum mechanical calculations.[59] The work reported herein extends the knowledge of the behaviour of this species. We devised a method for resolving the strong overlapping absorption and fluorescence spectra of the imidazolium and pyridinium cations found in equilibrium for **1-OMe**. This allowed us to estimate the ground-state equilibrium constant between them. Moreover, we were able to demonstrate the photobasic character of the pyridine nitrogen of **1-OMe** in the excited state.

2. Experimental

2.1 Synthesis and characterization

The compounds investigated in this work were prepared by the double condensation of a diamine and a carboxylic acid: 2,3-diaminopyridine and 2-methoxybenzoic acid (Aldrich) for **1-OMe** and 1-methyl-2-imino-1,2-dihydro-3-pyridinamine and salicylic acid for **1-NMe**. Polyphosphoric acid (Merck) was used as solvent and catalyst. The reaction mixture was heated to 160–180 ºC for 2 hours and the final products were washed with water several times and recrystallized from ethanol–water (50:50). 1-methyl-2-imino-1,2-dihydro-3-pyridinamine was synthesized as follows: 2,3-diaminopyridine was heated to 60 ºC for 1 minute in acetic anhydride (Aldrich) to yield 2,3-pyridinedicarbamic acid, which was refluxed for 4 hours in ethanol with an excess of methyl iodide (Aldrich). The reaction product, 2,3-bis(carboxyamino)-1-methylpyridinium iodide, was then heated to 90º C in 1 M hydrochloric acid for 40 minutes. The reaction mixture was basified with Na_2CO_3 and the solid precipitate obtained (1-methyl-2-imino-1,2-dihydro-3-pyridinamine) was filtered and washed. The structure of the new compound **1-NMe** was confirmed by high-resolution mass spectrometry (ESI-TOF; *m/z*: calculated for $C_{13}H_{12}N_3O^+$ ($[M+H]^+$) 226.0980, found 226.0979) and by ^{1}H–NMR (300 MHz; dimethyl sulfoxide–d_6; Me_4Si), δ/ppm: 4.30 (3 H, s), 6.92 (1 H, t, J = 7.82 Hz), 6.94 (1 H, d, J = 7.82 Hz) 7.30 (2 H, m), 8.28 (3 H, m)

The spectral properties of synthesized **1-OMe** compare favourably with those previously described for this compound.[59] ^{1}H–NMR of **1-OMe** (300 MHz, dimethyl sulfoxide–d_6; Me_4Si), δ (ppm): 3.95 (s, 1.2 H), 4.02 (s, 1.8 H), 7.05–7.28 (m, 3.4 H), 7.5 (m, 1 H), 7.92 (dd, 0.5 H, J = 1.42 Hz, J = 7.82 Hz), 8.02 (d, 0.3 H, J = 7.82 Hz), 8.20 (d, 0.3 H, J = 7.82 Hz), 8.30 (m, 1.6 H). The NMR spectrum reveals that **1-OMe** experiences a slow tautomeric equilibrium in dimethyl sulfoxide. Detailed data for this equilibrium was obtained by

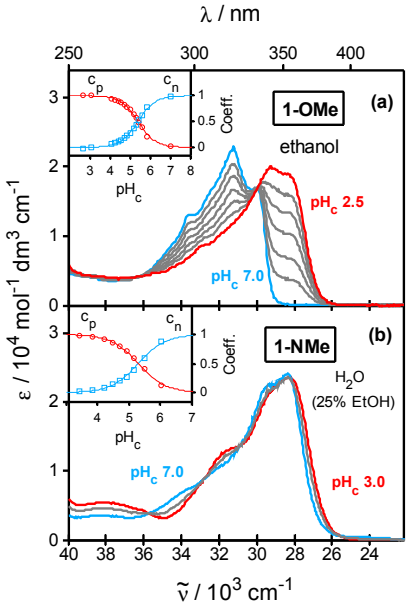

Fig. 2 (a) Absorption spectra of **1-OMe** in ethanol at various pH_c values between 2.5 and 7.0, [**1-OMe**] = 4.58 x 10^{-5} mol dm^{-3}. (b) Absorption spectra of **1-NMe** in water (25% ethanol) at various pH_c values between 3.0 and 7.0, [**1-NMe**] = 3.52 x 10^{-5} mol dm^{-3}. The insets show the experimental (symbols) and calculated (solid lines) acidity-dependent contributions of the protonated (c_p) and neutral (c_n) species.

Barraclough *et al.*[60] for the closely related species 2-(2',4'-dimethoxyphenyl)imidazo[4,5-*b*]pyridine in the same solvent. A comprehensive ^{13}C NMR investigation led these authors to conclude that a slow 1*H*–3*H* tautomerism with concomitant rotation about the C(2)–C(1') bond takes place, giving rise to the equilibrium of the two intramolecularly hydrogen-bonded tautomers N–H···OCH_3 in 2:1 proportion, favouring the 1*H*-tautomer. As judged by the relative intensities of the ^1H–NMR signals assigned to the methoxy group of **1-OMe** (1.8:1.2), the tautomers ratio would be (1.5:1) for this species in dimethyl sulfoxide. The rate of tautomerisation was found to be much faster in D_2O.[60]

2.2 Methods

Solutions were made up in double-distilled water treated with $KMnO_4$ and in spectroscopy-grade solvents. Aqueous solutions always contained 25% (v/v) ethanol, due to the low solubility of the compounds in pure water. Acidity was varied with $HClO_4$ (Fluka, 60%) in acetonitrile (Scharlau, 99.9%) and ethanol (Scharlau, 99.9%), and with NaOH (Fluka, 98%), $HClO_4$ and acetic acid/sodium acetate (Scharlau, 99.8%) or ammonium perchlorate/ammonia (Fluka, 98%) buffers in aqueous solutions. In all the solvents, pH_c was calculated as -log ([H^+]/mol dm^{-3}). All experiments were carried out at 20 °C and the solutions were not degassed.

UV–Vis absorption spectra were recorded in a Varian Cary 3E spectrophotometer. Fluorescence excitation and emission spectra were recorded in a Jobin Yvon–Spex Fluoromax-2 spectrofluorometer, with correction for instrumental factors by means of a reference photodiode and correction files supplied by the manufacturer. Sample concentrations of ~10^{-5} mol dm^{-3} for absorption and ~10^{-6} mol dm^{-3} for fluorescence were employed. Fluorescence quantum yields were measured using quinine sulphate (< 3 × 10^{-5} mol dm^{-3}) in aqueous H_2SO_4 (0.5 mol dm^{-3}) as standard (Φ = 0.546).[61, 62] Fluorescence lifetimes were determined by single-photon timing in an Edinburgh Instruments LifeSpec-ps spectrometer provided with three excitation sources: one diode laser at 375 nm and two light-emitting diodes (LEDs) at 333 nm and 308 nm. The equipment time resolution was ~ 20 ps with the diode laser and ~ 50 ps with the LEDs.

Model equations were fitted to the experimental data using a nonlinear weighted least-squares algorithm. All the data analysis (simple equation fitting, decay traces reconvolution and principal component global analysis) was performed with laboratory-made routines deployed in Matlab 7.5.0 for Windows. Taking into account all the experimental error sources, the standard uncertainty was estimated to be around 0.05 ns for the fluorescence decay times, 10% for the fluorescence quantum yields and 0.10 for ground-state pK_a measurements.

3. Results

3.1 Absorption spectra

The absorption spectra of **1-OMe** in ethanol at several acidities are shown in Fig. 2 (a). The absorption spectrum obtained under neutral conditions presented vibronic structure and peaked at 31300 cm^{-1}. Upon increasing the acidity, the spectra lost some vibronic structure and shifted to the red, the new maximum with similar intensity being located at 29500 cm^{-1}. The spectral characteristics observed for **1-OMe** in aqueous solution and ethanol were very alike.

Fig. 2 (b) shows some absorption spectra recorded for **1-NMe** in neutral-to-acid aqueous solution with 25% ethanol. The absorption spectrum in neutral medium presented its maximum at 28330 cm^{-1}. Acidification of the solution produced only a very slight change in the absorption spectrum, its maximum in acidic medium being located at 28250 cm^{-1}. The absorption spectra of **1-NMe** in ethanol and water were very alike.

3.2 Fluorescence spectra and lifetimes in neutral media

The absorption and fluorescence spectra of **1-OMe** in acetonitrile, ethanol, cyclohexane, and water with 25% ethanol were very similar, structured, and independent of the monitoring wavenumber (see the spectra in Fig. 3 (a) and (b) as representative examples). The fluorescence quantum yields were found to be quite high in all the solvents studied (Table 1). The fluorescence decay of **1-OMe** was monoexponential in the solvents just mentioned, the lifetime increasing in the series cyclohexane < acetonitrile < ethanol < water (Table 2).

The absorption spectrum of **1-OMe** in trifluoroethanol was very similar to that obtained in other solvents, but the fluorescence spectrum was very different, showing dual fluorescence (see panel (c) of Fig. 3). The normal Stokes-shifted band was very alike to the only band observed in other

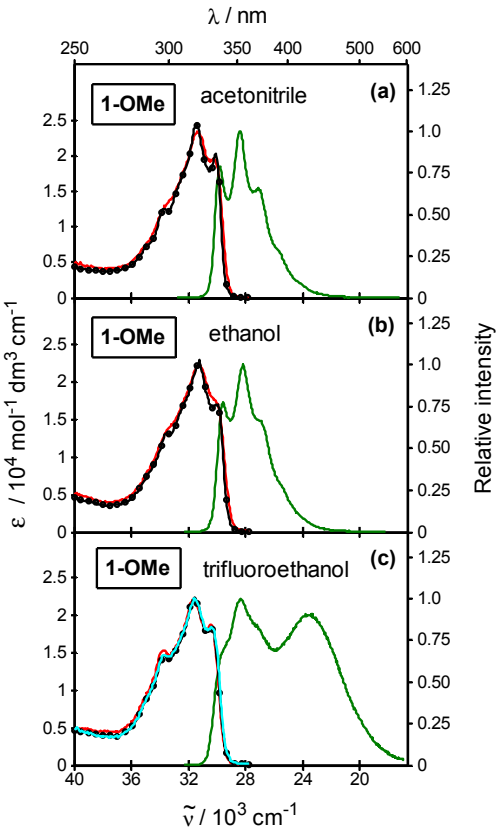

Fig. 3 Absorption spectra (—●—) and normalized fluorescence emission and excitation spectra of **1-OMe** in (a) acetonitrile, $\tilde{\upsilon}_{exc}$ = 33330 cm^{-1} (—), $\tilde{\upsilon}_{em}$ = 25640 cm^{-1} (—), (b) ethanol, $\tilde{\upsilon}_{exc}$ = 30300 cm^{-1} (—), $\tilde{\upsilon}_{em}$ = 27030 cm^{-1} (—), and (c) trifluoroethanol, $\tilde{\upsilon}_{exc}$ = 30300 cm^{-1} (—), $\tilde{\upsilon}_{em}$ = 27780 cm^{-1} (—), $\tilde{\upsilon}_{em}$ = 22220 cm^{-1} (—).

Table 1 Fluorescence quantum yields of **1-OMe** and **1-NMe** in various solvents at 298 K. The excitation wavenumbers are shown in parentheses

Solvent	Φ_F [**1-OMe**]	Φ_F [**1-NMe**]
	neutral media	
cyclohexane	—	very low
acetonitrile	0.48 (31750 cm^{-1})	very low
ethanol	0.56 (31750 cm^{-1})	very low
trifluoroethanol	0.52 (31750 cm^{-1})	0.035 (29410 cm^{-1})
water (25% EtOH)	0.64 (31750 cm^{-1})	very low
	acid media	
acetonitrile	0.54 (32260 cm^{-1})	0.17 (30770 cm^{-1})
	0.64 (28170 cm^{-1})	0.18 (29410 cm^{-1})
ethanol	0.66 (32260 cm^{-1})	very low
	0.71 (28170 cm^{-1})	
trifluoroethanol	0.55 (32260 cm^{-1})	0.15 (30770 cm^{-1})
	0.56 (29410 cm^{-1})	0.16 (29410 cm^{-1})
water (25% EtOH)	0.20 (32260 cm^{-1})	very low
	0.20 (29410 cm^{-1})	
	basic media	
water (25% EtOH)	—	very low

solvents. In addition, a new red-shifted emission band was observed with maximum at 23500 cm^{-1} and similar intensity to the normal Stokes-shifted band. The fluorescence quantum yield of **1-OMe** in trifluoroethanol had a similar value to those observed in other solvents (Table 1). The fluorescence decay of **1-OMe** in trifluoroethanol was found to be triexponential at both emission bands (Table 2).

No emission could be detected for **1-NMe** in neutral solvents, except for trifluoroethanol, where a very weak fluorescence was detected with emission maximum at 23260 cm^{-1} (Table 1). The fluorescence spectrum of **1-NMe** in trifluoroethanol overlapped the absorption spectrum and did not depend on the monitoring wavelength.

3.3 Fluorescence spectra and lifetimes in acid media

The fluorescence spectra of **1-OMe** in acidified acetonitrile and water with 25% ethanol exhibited similar features (panels (a) and (b) of Fig. 4). In both solvents, the fluorescence emission and excitation spectra were dependent of the monitoring wavenumber. When monitored at the blue-side of the emission spectrum, the excitation spectrum showed a two-band structure and was blue-shifted compared to the absorption spectrum recorded in the same conditions. In contrast, when monitored at the red side, the excitation spectrum was more similar to the first absorption band. The maximum of the emission band slightly shifted to the red as the excitation wavenumber decreased (for example, in acetonitrile from 23260 cm^{-1} with excitation at 32260 cm^{-1} to 22990 cm^{-1} with excitation at 28170 cm^{-1}). The fluorescence spectra of **1-OMe** in acidified trifluoroethanol and ethanol exhibited very similar features to those observed in acetonitrile and water with 25% ethanol.

The fluorescence quantum yield of **1-OMe** in acidified acetonitrile and ethanol varied with the excitation wavenumber, showing higher values when the excitation wavenumber decreased. On the contrary, the quantum yield was almost independent of the excitation wavenumber for **1-OMe** in trifluoroethanol and water with 25% ethanol (Table 1). The fluorescence decays of **1-OMe** in acidified media were biexponential in all the solvents studied. The relative contributions of the two lifetimes changed systematically with the emission wavenumber (Table 2).

The fluorescence of **1-NMe** in acidified media depended strongly on the nature of the solvent. No fluorescence emission could be detected in ethanol and water with 25% ethanol. On the contrary, a moderately intense fluorescence was observed in acidified acetonitrile and trifluoroethanol (see the quantum yields in Table 1). The absorption and fluorescence spectra of **1-NMe** in these solvents are presented in parts (c) and (d) of Fig. 4. The fluorescence spectra were similar in both solvents, showing a single emission band independent of the excitation wavenumber with maximum at ~22700 cm^{-1}. The excitation spectrum was independent of the monitoring wavenumber and its maximum coincided with that of the absorption spectrum. Nevertheless, in neither solvent did the shape of the excitation spectra match the shape of the absorption spectra, which were in turn very similar in all the solvents investigated.

Table 2 Fluorescence decay times τ of compounds **1-OMe** and **1-NMe** in various solvents at 298 K, obtained by global analysis of the decays at the indicated emission wavenumbers. When a multi-exponential decay function was fitted, it is indicated at each wavenumber the pre-exponential factor B and the associated percentage (in parentheses) of each exponential term. Shown in square brackets are the species to which each lifetime was assigned. The excitation wavenumber was 32470 cm^{-1} for **1-OMe** and 26670 cm^{-1} for **1-NMe.**

Solvent	$\tilde{\upsilon}_{em}$/ cm^{-1}	τ_1 / ns {B_1 (%)}	τ_2 / ns {B_2 (%)}	τ_3 / ns {B_3 (%)}	χ^2
		1-OMe in neutral media			
cyclohexane	28570, 27030	0.81 $[\mathbf{N_i^*}]$			1.068
acetonitrile	28570, 27030	1.19 $[\mathbf{N_i^*}]$			1.033
ethanol	28570, 27030	1.36 $[\mathbf{N_i^*}]$			1.031
trifluoroethanol	29410–22730	1.16 $[\mathbf{N_i^*}]^a$	4.99 $[\mathbf{C_p^*}]$	0.48 $[\mathbf{N_i^*}]^a$	1.040
	29410	{266 (73%)}	{2 (2%)}	{217 (25%)}	1.124
	27780	{268 (71%)}	{4 (4%)}	{223 (25%)}	1.036
	26320	{288 (57%)}	{33 (29%)}	{173 (14%)}	1.028
	25000	{255 (23%)}	{191 (75%)}	{54 (2%)}	0.963
	23810	{148}	{434}	{-135}	1.039
	22730	{39}	{558}	{-228}	1.049
water (25% EtOH)	28570, 27030	1.75 $[\mathbf{N_i^*}]$			1.020
		1-OMe in acidic media			
acetonitrile (pH_c 2.8)	27030–22220	2.51 $[\mathbf{C_i^*}]$	4.97 $[\mathbf{C_p^*}]$		1.043
	27030	{465 (91%)}	{24 (9%)}		1.050
	25640	{373 (62%)}	{115 (38%)}		1.070
	24390	{222 (30%)}	{268 (70%)}		1.036
	23260	{101 (12%)}	{389 (88%)}		1.019
	22220	{38 (4%)}	{451 (96%)}		1.038
ethanol (pH_c 2.0)	27030–22220	2.33 $[\mathbf{C_i^*}]$	4.27 $[\mathbf{C_p^*}]$		1.059
	27030	{442 (82%)}	{52 (18%)}		1.061
	25640	{319 (49%)}	{179 (51%)}		1.026
	24390	{181 (24%)}	{307 (76%)}		1.059
	23260	{90 (11%)}	{404 (89%)}		1.116
	22220	{33 (4%)}	{459 (96%)}		1.034
trifluoroethanol (pH_c 3.0)	27030–22220	2.51 $[\mathbf{C_i^*}]$	5.14 $[\mathbf{C_p^*}]$		1.056
	27030	{440 (81%)}	{51 (19%)}		1.156
	25640	{355 (56%)}	{136 (44%)}		1.055
	24390	{234 (31%)}	{254 (69%)}		1.023
	23260	{129 (15%)}	{357 (85%)}		1.008
	22220	{58 (6%)}	{424 (94%)}		1.031
water (25% EtOH, pH_c 1.0)	26320–23810	1.96 $[\mathbf{C_i^*}]$	1.72 $[\mathbf{C_p^*}]$		1.062
	26320	{482 (99%)}	{6 (1%)}		1.061
	25000	{432 (91%)}	{48 (9%)}		1.085
	23810	{310 (66%)}	{178 (34%)}		1.041
		1-NMe in acidic media			
acetonitrile (pH_c 2.8)	25000–20830	1.65 [$\mathbf{C_p 3}\boldsymbol{H^*_{syn}}$ or/and $\mathbf{C_p 1}\boldsymbol{H^*_{anti}}$]			1.106

[a] Decay times associated with the decay of these species, probably non-exponential due to several steps of geminate protonation–deprotonation by the solvent.

4. Discussion

4.1 Acid–base equilibria of 1-NMe and 1-OMe, and ground-state tautomeric equilibria for cationic 1-OMe

The absorption spectra of **1-NMe** shown in Fig. 2 (b) reveal that this species experiences an acid–base equilibrium in neutral-to-acid solutions, which must be assigned to the protonation of one of the imidazole-type nitrogens. The observed spectral changes are very small, as was also previously found for protonation of many benzimidazole derivatives.[63-65] In strongly basic media, an additional ground-state equilibrium was found (results not shown), which must correspond to the deprotonation of the OH group, the only acidic position of the molecule. The series of absorption spectra was analyzed by principal-component global analysis[66] to obtain the spectral components associated with the protonated (p), neutral (n) and deprotonated (d) forms of **1-NMe**, together with their experimental and calculated acidity-dependent spectral contributions c_p, c_n, and c_d (*cf.* inset in part (b) of Fig. 2), and the acidity constants calculated on a concentration basis. The pK_a value obtained for deprotonation in water was 12.92. The pK_a corresponding to the equilibrium between the protonated and the neutral form

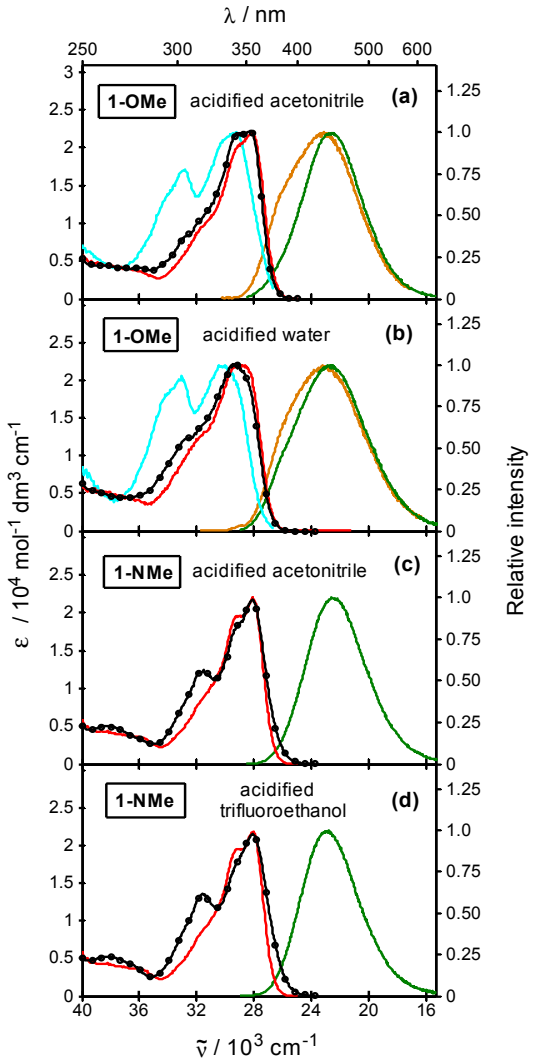

Fig. 4 Absorption spectra (—●—) and normalized fluorescence emission and excitation spectra of (a) **1-OMe** in acidified acetonitrile, [HClO4] = 1 ×10^{-3} mol dm^{-3}, $\tilde{\upsilon}_{exc}$ = 28990 cm^{-1} (—), $\tilde{\upsilon}_{exc}$ = 33330 cm^{-1} (—), $\tilde{\upsilon}_{em}$ = 26320 cm^{-1} (—), $\tilde{\upsilon}_{em}$ = 20830 cm^{-1} (—), (b) **1-OMe** in acidified water (25% ethanol) of pH_c 1.0, $\tilde{\upsilon}_{exc}$ = 28570 cm^{-1} (—), $\tilde{\upsilon}_{exc}$ = 33330 cm^{-1} (—), $\tilde{\upsilon}_{em}$ = 26320 cm^{-1} (—), $\tilde{\upsilon}_{em}$ = 20830 cm^{-1} (—), (c) **1-NMe** in acidified acetonitrile, [HClO4] = 1 ×10^{-3} mol dm^{-3}, $\tilde{\upsilon}_{exc}$ = 29420 cm^{-1} (—), $\tilde{\upsilon}_{em}$ = 22730 cm^{-1} (—) and (d) **1-NMe** in acidified trifluoroethanol, [HClO4] = 1 ×10^{-3} mol dm^{-3}, $\tilde{\upsilon}_{exc}$ = 29420 cm^{-1} (—), $\tilde{\upsilon}_{em}$ = 22730 cm^{-1} (—).

was 5.31 (Table 3).

The absorption spectra of **1-OMe** in ethanol at different acidities are shown in Fig. 2 (a). A ground-state equilibrium was found within the pH range 3–7. By applying principal component global analysis to the series of absorption spectra of **1-OMe**, we obtained the spectral components associated with the protonated (p) and neutral (n) forms, together with their experimental and calculated acidity-dependent spectral contributions c_p and c_n, (see inset in part (a) of Fig. 2), and the acidity constant pK_a shown in Table 3. The pK_a value obtained in the same way for **1-OMe** in water with 25% of ethanol

Table 3 Experimental values for the macroscopic acidity constants (pK_a) of protonated **1-OMe** and **1-NMe** in various solvents at 298 K, and estimated values of the equilibrium constant between imidazolium and pyridinium cations of **1-OMe** (K_{ip}) and microscopic acidity constants of each cation in the ground state (p$K_{a(i)}$ and p$K_{a(p)}$) and the first-excited singlet state (p$K^*_{a(i)}$ and p$K^*_{a(p)}$). Last columns list the hydrogen-bond donor (α) and hydrogen-bond acceptor (β) ability of the pure solvents.[67]

Solvent	pK_a	K_{ip}	p$K_{a(i)}$	p$K_{a(p)}$	p$K^*_{a(i)}$	p$K^*_{a(p)}$	α	β
			1-OMe					
Acetonitrile		8.8					0.19	0.31
Ethanol	5.40	5.6	4.6	5.3	8[a]	12[a]	0.83	0.77
Water (25% EtOH)	4.00	3.9	3.3	3.9	7[a]	10[a]	1.17	0.18
Trifluoroethanol		3.7					1.51	0
			1-NMe					
Water (25% EtOH)	5.31							

[a] Values calculated by using the Förster cycle method.

(4.00) is very similar to that reported by Dogra *et al* (4.1).[59]

1-OMe possesses two basic groups, the imidazole nitrogen and the pyridine nitrogen. As we stated before, protonation at the benzimidazole nitrogen hardly changes the absorption spectrum.[63-65] This was experimentally verified for **1-NMe**, as there is no significant shift between the spectrum of the neutral and protonated forms (*cf.* Fig. 2 (b)). Conversely, protonation at the pyridine or quinoline nitrogen in pyridylbenzimidazoles,[63, 64, 68] or quinoline derivatives[69, 70] produces generally a red shift of the absorption spectrum. As can be seen in Fig. 2 (a), the absorption spectrum of **1-OMe** in acid media is considerably red shifted with respect to the neutral form spectrum, indicating that protonation probably takes place to a great extent at the pyridine nitrogen. Moreover, the fluorescence spectra and lifetimes of **1-OMe** in acid media (to be discussed in the next section, *cf.* Fig. 4 (a) and (b) and Table 2) have led us to propose that two different monocations exist for **1-OMe** at equilibrium in the ground state. Scheme 1 presents the ground-state equilibria proposed for **1-OMe** in acid media. We designate the two protonated species as imidazolium cation ($\mathbf{C_i}$) and pyridinium cation ($\mathbf{C_p}$), and the corresponding microscopic acidity constants for each cation as $K_{a(i)}$ and $K_{a(p)}$. The neutral species is represented by the 1*H* tautomer with an intramolecular hydrogen bond, which is probably the most stable structure in polar solutions according to NMR results on related species[60] and quantum mechanical calculations,[59] but a considerable amount must also exist of the 3*H* tautomer, as was demonstrated in this work for **1-OMe** in dimethyl sulfoxide (see the experimental section) and for related species[60] in the same solvent. The cations $\mathbf{C_i}$ and $\mathbf{C_p}$ probably experience also a rotational isomerism, but the UV-Vis spectral properties of

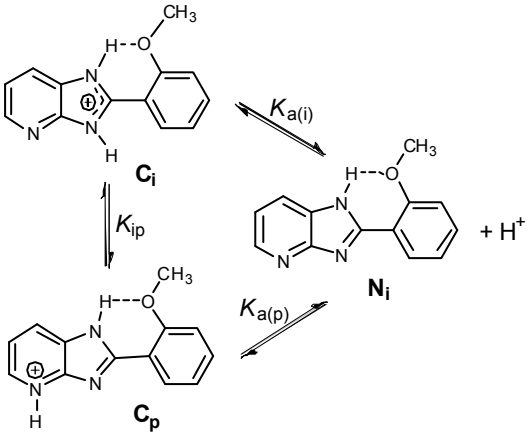

Scheme 1 Acid-base equilibria between neutral and cationic forms of **1-OMe**.

both rotamers, as those of the corresponding 1*H*–3*H* tautomers of $\mathbf{N_i}$, must be very similar.

The formation of the pyridinium cation is supported by the comparison of the spectra of **1-OMe** and **1-NMe** in acid media (Fig. 2), which show the first-band absorption in the same region. As the pyridinium cation $\mathbf{C_p}$ of **1-OMe** must have a very similar electronic structure to the protonated form of **1-NMe** (only hydrogen atoms replacing the methyl groups of each species), the similarity of the absorption spectra for **1-OMe** and **1-NMe** in acid media supports the assumption that **1-OMe** protonates to a great extent at the pyridinium nitrogen.

The measured macroscopic acidity constant K_a is related to the microscopic constants $K_{a(i)}$ and $K_{a(p)}$ by the equation:

$$\frac{1}{K_a} = \frac{1}{K_{a(i)}} + \frac{1}{K_{a(p)}} \quad (1)$$

Defining the equilibrium constant between the cations, K_{ip}, as the ratio between the concentrations of pyridinium and imidazolium cations, the following relation holds between K_{ip} and the microscopic acidity constants $K_{a(i)}$ and $K_{a(p)}$ (see Scheme 1):

$$K_{ip} = \frac{[\mathbf{C_p}]}{[\mathbf{C_i}]} = \frac{K_{a(i)}}{K_{a(p)}} \quad (2)$$

The microscopic constants $K_{a(i)}$ and $K_{a(p)}$ cannot be obtained spectrophotometrically, since the absorption spectra of the imidazolium and pyridinium cations cannot be recorded separately. As the macroscopic acidic constant K_a is experimentally measured, it is necessary to know one of the microscopic constants, $K_{a(i)}$, $K_{a(p)}$ or K_{ip}, to calculate the other two by equations 1 and 2. We estimated K_{ip} by fluorescence measurements, as will be described in the next section.

4.2 Interpretation of the absorption, fluorescence spectra and lifetimes of 1-OMe in acidic solutions: resolution of the strongly overlapping absorption and fluorescence spectra from pyridinium and imidazolium cations

Both the fluorescence excitation and emission spectra of **1-OMe** in acidic media depended on the monitoring wavenumber (*cf.* panels (a) and (b) of Fig. 4), indicating that there is more than one species present in both the ground and the excited states. This finding supports the hypothesis presented in last section that ground-state pyridinium and imidazolium cations coexist in equilibrium. The fluorescence emission spectra showed considerable overlap with the excitation spectra, suggesting that the excited and the emitting species are the same, *i.e.* the pyridinium and imidazolium cations. The biexponential fluorescence decays with positive amplitudes obtained for **1-OMe** in acidified acetonitrile, ethanol, trifluoroethanol and water with 25% ethanol (Table 2) support the proposal that two independent emitting species exist in solution.

We mentioned above that the first absorption band of the pyridinium cation must be significantly red shifted with respect to that of the imidazolium cation. Therefore, the red-shifted excitation spectrum, which was obtained by monitoring at the red tail of the emission spectrum of **1-OMe** in acid media (*cf.* parts (a) and (b) of Fig. 4), must have a larger contribution from the pyridinium cation $\mathbf{C_p}$ spectrum; conversely, the blue-shifted excitation spectrum, monitored at the higher-energy end of the emission spectrum, must include a major contribution from the imidazolium cation $\mathbf{C_i}$. The higher fluorescence quantum yield values obtained by exciting protonated **1-OMe** in acetonitrile or ethanol at the red end of the absorption spectrum (Table 1) indicate therefore that the pyridinium cation has a higher fluorescence quantum yield than the imidazolium cation in these solvents.

To throw light on the ground-state equilibrium between pyridinium and imidazolium cations, series of fluorescence excitation spectra were recorded for **1-OMe** in several acidified solvents at different emission wavelengths, from 360 nm to 490 nm in steps of 5 nm (a total of 27 excitation spectra for each solvent). Assuming that the fluorescent species in sufficiently acidified media are indeed $\mathbf{C_i^*}$ and $\mathbf{C_p^*}$, any excitation spectra $\mathbf{E}$ should be the sum of contributions from $\mathbf{C_i^*}$ and $\mathbf{C_p^*}$ excitation spectra ($\mathbf{E}_{C_i}$ and $\mathbf{E}_{C_p}$ respectively, see equation 3).

$$\mathbf{E} = c_{C_i}\mathbf{E}_{C_i} + c_{C_p}\mathbf{E}_{C_p} \quad (3)$$

In this equation, the coefficients c_{C_i} and c_{C_p} represent the relative contributions from $\mathbf{C_i^*}$ and $\mathbf{C_p^*}$ spectra to any experimental excitation spectrum at the corresponding emission wavelength. A principal component analysis of the experimental series indicated that two independent spectral components are needed to reproduce the fluorescence excitation spectra of **1-OMe** in different acidified media, confirming the proposal of eqn (3). The coefficients c_{C_i} and c_{C_p} are proportional to the amount of photons emitted by each species at the corresponding emission wavelength, which in turn is modulated by the shape of the fluorescence emission spectra of each species. The unstructured emission spectra shown Fig. 4 (a) and (b) allow us to assume that the fluorescence emission spectra of $\mathbf{C_i^*}$ and $\mathbf{C_p^*}$ will properly fit to log-normal functions.[71] Therefore, a principal component global analysis[66] was performed on the fluorescence excitation spectral series, assuming that the wavenumber dependence of the coefficients c_{C_i} and c_{C_p} follows a log-normal distribution. In the fitting process, the component excitation spectra $\mathbf{E}_{C_i}$ and $\mathbf{E}_{C_p}$ are obtained, as well as their experimental and calculated contributions c_{C_i} and c_{C_p} (see Fig. 5). The experimental excitation spectra of **1-OMe** at any emission

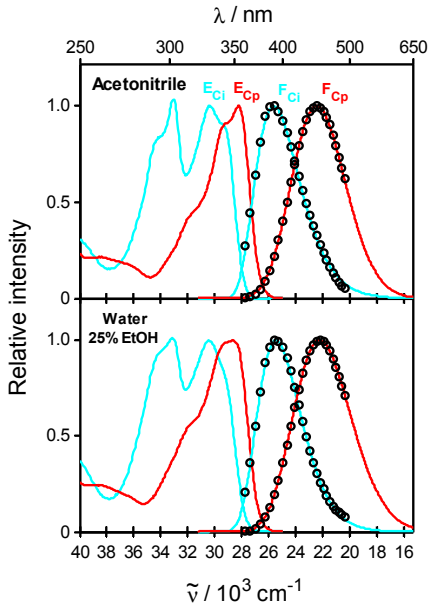

Fig. 5 Normalized fluorescence excitation ($\mathbf{E}_{C_i}$ and $\mathbf{E}_{C_p}$) and emission ($\mathbf{F}_{C_i}$ and $\mathbf{F}_{C_p}$) spectra of the imidazolium (—) and pyridinium (—) cations of **1-OMe** in acidified acetonitrile and water (25% ethanol). The excitation spectra were obtained as component spectra in a principal component global analysis of a series of 27 excitation spectra at different emission wavenumbers. The analysis also yielded the wavenumber-dependent coefficients (**o**) of the component spectra. The fitting of a log-normal function to these coefficients provided the emission spectra.

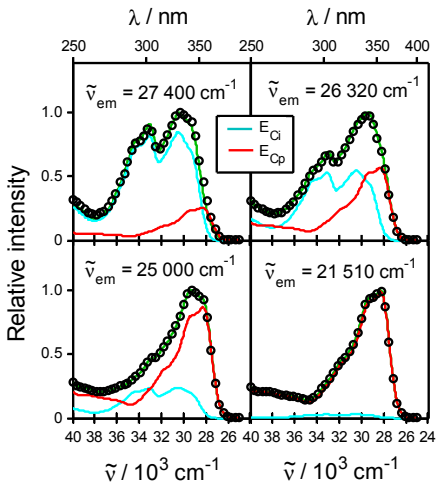

Fig. 6 Normalized experimental (—) and calculated (**o**) fluorescence excitation spectra of **1-OMe** in acidified ethanol at different emission wavenumbers. The calculated spectra were obtained as linear combination of the component excitation spectra associated to the imidazolium (—) and pyridinium (—) cations, whose individual contributions are also shown. Principal component global analysis of a series of 27 excitation spectra provided the imidazolium and pyridinium cations component spectra.

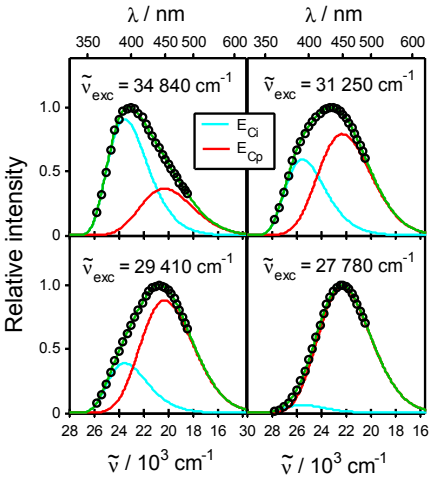

Fig. 7 Normalized experimental (**o**) and calculated (—) fluorescence emission spectra of **1-OMe** in acidified water with 25% ethanol at different excitation wavenumbers. The calculated spectra were obtained by fitting a linear combination of the imidazolium (—) and pyridinium (—) cation emission spectra obtained by principal component global analysis as described in Section 4.2 and Fig. 5.

wavelength are well fitted by this model (see in Fig. 6 the results for ethanol; similar results were obtained for the rest of the solvents). The excitation spectra $\mathbf{E}_{C_i}$ and $\mathbf{E}_{C_p}$ obtained in the analysis differ markedly in shape and position of the band maxima and bear, as expected, some resemblance to the experimental excitation spectra obtained at the red and blue side of the **1-OMe** emission spectrum (Fig. 4).

The fitting and extrapolation of a log-normal function to the coefficients c_{C_i} and c_{C_p} obtained from the principal component global analysis yielded the individual fluorescence emission spectra of each cation, $\mathbf{F}_{C_i}$ and $\mathbf{F}_{C_p}$. Fig. 5 shows the results obtained in acidified acetonitrile and water with 25% ethanol. The experimental fluorescence emission spectra of **1-OMe** in acidified solvents could be satisfactorily reproduced by a linear combination of $\mathbf{F}_{C_i}$ and $\mathbf{F}_{C_p}$. The good quality of the fit for acidified water with 25% ethanol can be seen in Fig. 7 at several excitation wavenumbers.

Once the excitation spectra of $\mathbf{C}_i^*$ and $\mathbf{C}_p^*$ were known, we tried to reproduce the experimental absorption spectrum of **1-OMe** in acidified media as a linear combination of $\mathbf{E}_{C_i}$ and $\mathbf{E}_{C_p}$. The results are shown in Fig. 8, where the contribution from each cation to the absorption spectrum of **1-OMe** in various acidified solvents and the goodness of the fits can be appreciated. An excellent agreement is found between the spectra calculated by the method described and the experimental absorption spectra, which confers additional support to the analysis performed.

Fig. 8 shows graphically that the contribution from the pyridinium cation to the first absorption band of **1-OMe** is greater than that of the imidazolium cation in all the solvents studied, the latter having a maximum contribution in trifluoroethanol and minimum in acetonitrile. The determination of the equilibrium constant between the cations from the spectral contributions shown in Fig. 8 requires knowing the molar absorption coefficient of one cation at

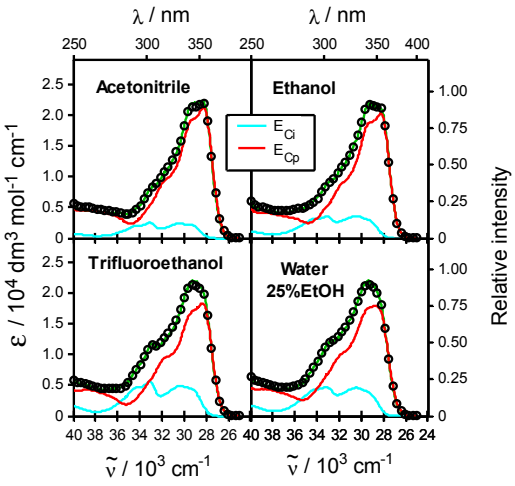

Fig. 8 Experimental (—) and calculated (**o**) absorption spectra of **1-OMe** in different acidified media. Principal component global analysis of a series of 27 excitation spectra collected at different emission wavenumbers provided the imidazolium (—) and pyridinium (—) cations excitation spectra, whose linear combination was fitted to the experimental absorption spectra.

some wavelength. Our results do not allow obtaining this datum, as both cations are always present in comparable amounts in solution. We can make nevertheless a reasonable guess for the maximum molar absorption coefficients of the cations at the first absorption band (ε_{max}), based on the following data:

(i) for many benzimidazole derivatives, protonation at the benzimidazole nitrogen doesn't change ε_{max}.[63-65] The spectra of **1-NMe** proved this assertion (see part (b) of Fig. 2). Based on these facts, we anticipate for the imidazolium cation of **1-OMe** a similar ε_{max} to the neutral form;

(ii) the chemical structure of the **1-OMe** pyridinium cation is very similar to that of the only cation of **1-NMe** (only hydrogen atoms replacing methyl groups in each other's structure), so we expect a similar ε_{max} for both cations;

(iii) the ε_{max} values for **1-OMe** and **1-NMe**, both in neutral and acidic solutions in different solvents, are very similar (see Fig. 2).

These facts led us to assume that ε_{max} is similar for the imidazolium and pyridinium cations of **1-OMe**. Under this approximation, from the ratio of maximum absorbances of the pyridinium and imidazolium cations in the spectral decompositions of Fig. 8, we can estimate the equilibrium constant between the cations (K_{ip}) in the solvents studied. The estimated values (Table 3) show that the fraction of pyridinium cation is always much greater than that of the imidazolium cation in the solvents studied here. This result is in keeping with the predominant protonation at the pyridine nitrogen found for the closely related species 2-(2',4'-dimethoxyphenyl)imidazo[4,5-*b*]pyridine by ^{1}H NMR measurements.[60]

The estimated K_{ip} values for **1-OMe** decrease in the order acetonitrile > ethanol > water > trifluoroethanol (Table 3). This means that the fraction of pyridinium cation $\mathbf{C_p}$ reaches a maximum in acetonitrile (see Fig. 8). The dipolar solute-solvent interactions do not seem to be the main factor affecting this trend, as the dielectric constant of acetonitrile has an intermediate value between water and the alcohols, and the more polar pyridinium cation should become more stabilized in water than in acetonitrile by dipolar interactions. To test whether the hydrogen-bond interactions are the key factors determining the relative stability of the cations in the different solvents, we examined the values of the parameters representing the hydrogen-bond donor (α) and the hydrogen-bond acceptor (β) ability of the solvent, listed in Table 3.[67] It is observed that the K_{ip} values of **1-OMe** decrease as α increases, showing in turn no correlation with β. This means that the fraction of imidazolium cation reaches a maximum in trifluoroethanol, the solvent with the highest hydrogen-bond donor ability. Since $\mathbf{C_i}$ and $\mathbf{C_p}$ isomers of **1-OMe** differ only in the kind of nitrogen available for accepting a hydrogen bond from the solvent (see Scheme 1), we can conclude that the hydrogen-bond donor interaction of the solvent with the pyridine nitrogen must be very strong and the key factor contributing to the relative stabilization of the imidazolium cation in hydrogen-bonding solvents.

The experimental pK_a values for **1-OMe** in ethanol and water, together with the estimated K_{ip} values, allow for the determination of the microscopic acidity constants $K_{a(i)}$ and $K_{a(p)}$ by using eqns. (1) and (2). The values obtained, listed in Table 3, show that the pyridine nitrogen is slightly more basic than the imidazole nitrogen for **1-OMe**. An estimation of the acidity constants in the first-excited singlet state can be obtained by the Förster cycle method.[72] As the spectra do not show vibrational structure, the energy of the (0,0) band was estimated by the intersection point between the normalized excitation and emission fluorescence spectra of each species.[73] The pK_a^* values obtained (*cf.* Table 3) indicate that the pyridine nitrogen becomes much more basic in the excited state, showing a strongly photobasic character with an increase in the pK_a of more than 6 units upon excitation. The imidazole nitrogen is also more basic in the excited state, but the basicity increase is much smaller than that of the pyridine nitrogen.

Some insight into the electronic properties of the species studied might be obtained by a comparison of the pK_a values with those of related molecules. The p$K_{a(i)}$ value for **1-OMe** in water (3.3) is nearly 2 units lower than that for 2-(2'-methoxyphenyl)benzimidazole (5.1),[74] which lacks the pyridine nitrogen of **1-OMe**. This result shows that the pyridine nitrogen has a strong electron-withdrawing effect, enhancing the acidity of the imidazolium cation of **1-OMe**.

The pK_a value obtained for protonated **1-NMe** (5.31) is significantly higher than that corresponding to the pyridinium cation of **1-OMe** (3.9). Since the protonated form of **1-NMe** has formally the same electronic structure as the pyridinium cation $\mathbf{C_p}$, the lower resonance energy and consequent higher energy content of neutral **1-NMe** compared to neutral **1-OMe** could explain the weaker acidity of the **1-NMe** cation. In the same way, the measured pK_a value for OH-deprotonation of **1-NMe** (12.92) is much higher than the value obtained for the non-methylated parent molecule 2-(2'-hydroxyphenyl)imidazo [4,5-*b*]pyridine (8.6),[75] indicating a lower capacity of **1-NMe**

anion to stabilize the negative charge through resonance effects and the formation of an intramolecular hydrogen bond N–H···O⁻.

The fluorescence decay of protonated **1-OMe** is biexponential (Table 2). At the red end of the emission spectrum, the longer lifetime shows its maximum relative contribution to the fluorescence decay in acetonitrile, ethanol and trifluoroethanol. This lifetime (4–5 ns) has therefore to be assigned to the pyridinium cation, and the shorter lifetime (2.3–2.5 ns) to the imidazolium cation.

The fluorescence properties of **1-OMe** were similar in acidic aqueous solution (25% EtOH) and in the rest of the solvents, only a lower quantum yield (Table 1) and shorter lifetimes (Table 2) being noticed as distinctive differences. In contrast to other solvents, the longest fluorescence lifetime in water (1.96 ns) shows its maximum contribution to the decay at the higher-energy side of the emission spectrum (Table 2), indicating that this decay time has to be attributed to the imidazolium cation. The shorter lifetime (1.72 ns), with maximum contribution at lower wavenumbers, has to be assigned to the pyridinium cation. Comparison of these lifetimes with those found in other solvents (Table 2) shows that the excited-state lifetime of the imidazolium cation is only a bit shorter in aqueous solution than in other solvents, but the pyridinium lifetime is much shorter in aqueous solution. As the spectra are similar in all the solvents, these results suggest that the radiationless deactivation of the pyridinium cation is much faster in aqueous solution than in other solvents. This fact is probably the main reason for the lower fluorescence quantum yield of protonated **1-OMe** in water relative to other solvents (Table 1).

4.3 Excited-state behaviour of 1-OMe in neutral solutions: photobasic properties of the pyridine nitrogen

The fluorescence properties of **1-OMe** were very similar for all the solvents studied except trifluoroethanol, which will be discussed later. The following experimental results are important for the discussion: (a) similar fluorescence excitation and emission spectra with small Stokes shift were obtained for **1-OMe** in all the solvents examined (Fig. 3); (b) the excitation and emission spectra were independent of the monitoring wavenumber; (c) the excitation spectrum perfectly matched the absorption spectrum; (d) a monoexponential fluorescence decay was observed in all the solvents (Table 2).

The fluorescence behaviour of **1-OMe** just described suggests that only one absorbing and emitting species exists in the solvents mentioned. The well-resolved vibronic structure and mirror-image relationship of the absorption and fluorescence spectra suggests that this species has a planar configuration in both the ground and the excited states, since loss of planarity in this kind of molecules gives rise to a large hypsochromic shift and loss of vibrational structure.[76-79] In Fig 1, we represent neutral **1-OMe** by the $\mathbf{N_i}$ structure, but we don't know the main conformation of this species in solution, as the benzimidazole hydrogen could be attached to the N(1) or N(3) position, and the methoxyphenyl group could be rotated. The fluorescence measurements seem to indicate that one of these conformations is in much greater concentration than the others, but our results do not allow finding out which one is the main conformation.

The absorption and fluorescence spectra of neutral **1-OMe** in acetonitrile, ethanol and water were very alike (see Fig. 3), this fact indicating a constant value of the radiative deactivation constant in these solvents. Nevertheless, both the fluorescence quantum yields and lifetimes increase in the series acetonitrile < ethanol < water (25% EtOH), the increase in the lifetime value being larger than in the quantum yield value. These facts imply that a decrease in the radiationless deactivation constant takes place in the series acetonitrile > ethanol > water (25% EtOH), as has already been found in a previous investigation.[59] The data obtained suggest that the hydrogen-bond interactions with the solvent molecules induce this decrease in the radiationless deactivation rate constant.

1-OMe showed dual fluorescence in trifluoroethanol (panel (c) of Fig. 3). In addition to the normal Stokes-shifted band also observed in other solvents, a new large Stokes-shifted emission appeared with almost the same intensity. The excitation spectra obtained at both emission bands were identical, matching perfectly the absorption spectrum of **1-OMe**. This finding shows that both emission bands derive from the same ground-state precursor. The great similarity of the absorption spectra in all the solvents examined (*cf.* Fig. 3) strongly supports that this precursor must be the neutral form of **1-OMe**, no absorption by different species being detected.

Investigations on several pyridyl derivatives of benzimidazole and related molecules have shown that the pyridine nitrogen strongly increases its basicity on excitation, becoming protonated even by water in neutral medium.[63, 68, 80, 81] No such behaviour was observed for the benzimidazole nitrogens, which do not show detectable photobasic properties.[68] Based on these facts, we expected for **1-OMe** a strongly increased basicity of the pyridine nitrogen in the excited state. The excited-state acidity constants estimated by the Förster cycle method (Table 3) confirm this hypothesis, as they predict more than 6 units increase in the $pK_{a(p)}$ of the pyridinium cation upon excitation, but only 3-4 units increase for the $pK_{a(i)}$ of the imidazolium cation of **1-OMe**. This means that an acidic solvent like trifluoroethanol (pK_a 12.37),[82] will probably be able to protonate the pyridine nitrogen of **1-OMe** in the excited state. According to this hypothesis, the red-shifted band and the long fluorescence lifetime showing maximum amplitude at lower wavenumbers (4.99 ns, Table 2) have to be assigned to the emission of the pyridinium cation $\mathbf{C_p^*}$ of **1-OMe**, formed by protonation in the excited state of the neutral molecule. This assignment is supported by the measurements carried out in acidified trifluoroethanol (see above), which showed an emission with similar features and lifetime (5.14 ns, Table 2), assigned to the pyridinium cation.

Scheme 2 summarizes the proposed excitation and deactivation pattern for **1-OMe** in trifluoroethanol solution. The excited non-protonated molecules of **1-OMe** would emit the normal Stokes-shifted emission band (~ 28400 cm^{-1}), very similar to the fluorescence measured in non-acidic solvents like acetonitrile or ethanol (*cf.* Fig. 3). The fluorescence decay of this band was found to be triexponential in trifluoroethanol (Table 2). The longest decay (4.99 ns), with very low

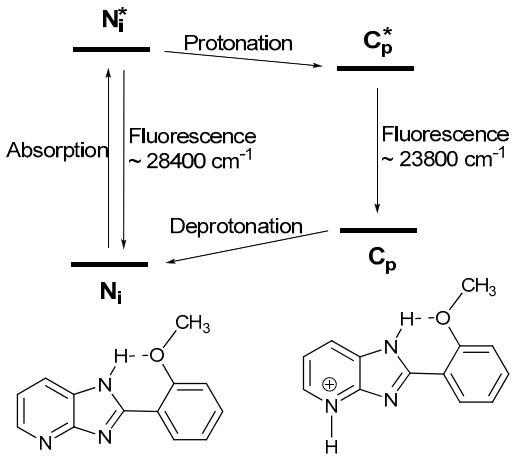

Scheme 2 Excitation and deactivation pattern proposed for **1-OMe** in neutral trifluoroethanol solution.

contribution, must correspond to the red-shifted pyridinium band tail, but the two shorter lifetimes (1.16 ns and 0.48 ns), with maximum contribution on the blue side of the emission spectrum, have to be associated with the decay of the excited neutral species. The pre-exponential factors of these lifetimes are positive at wavelengths corresponding to the normal Stokes-shifted band, decreasing with wavenumber and reaching negative values for the shorter lifetime at the lowest wavenumbers. This is an indication that the pyridinium cation emitting at low wavenumbers is formed in the excited state from species emitting at the normal Stokes-shifted band. Nevertheless, a simple scheme of one-step protonation of the neutral molecule by the solvent would not explain the triexponential fluorescence decay. The coexistence in the excited state of both the neutral and the protonated pyridinium forms of **1-OMe** in trifluoroethanol means that probably the protonation process is reversible, due to similar basicities of solute and conjugate base of the solvent. In this case, several steps of geminate protonation–deprotonation of excited **1-OMe** by the solvent would probably take place, as it has been thoroughly studied for the analogous processes of photoacid deprotonation by the solvent.[83, 84] This scheme leads to time-dependent rate constants and non-exponential decays. If the same behaviour holds for photoprotonation of the neutral form of **1-OMe**, the triexponential fit would give only an approximation to the real decay.

The fact that the fluorescence quantum yields of **1-OMe** show comparable values in trifluoroethanol and the rest of the solvents studied (Table 1) indicates that the neutral form of **1-OMe** and its pyridinium cation have similar quantum yields. Consequently, the similar intensities of the fluorescence bands associated with these species imply that both are present in comparable amounts in the excited state in trifluoroethanol.

4.4 Excited-state behaviour of 1-NMe in neutral solutions: proton-coupled charge-transfer hypothesis (ESIPT-TICT mechanism)

1-NMe in neutral media showed no detectable fluorescence emission except in trifluoroethanol, where a weak fluorescence could be detected (Table 1). As fluorescence is the main technique we used to study the excited-state properties, we have no direct information on the fate of excited **1-NMe** in these media. Nevertheless, based on the behaviour of structurally related molecules, we will propose a hypothesis for the lack of fluorescence.

The most stable structure of **1-NMe** is probably that depicted in Scheme 3 as the planar $\mathbf{N_p}$ form or its conformational isomer with 180° rotation around the interannular bond. They both present an intramolecular hydrogen bond between the hydroxyl group and the imidazole nitrogen. Taking into account the known photoacid character of the hydroxyl group and the behaviour of a large number of similar molecules,[1-5] $\mathbf{N_p^*}$ probably experiences an ultrafast ESIPT process to yield the tautomeric form $\mathbf{T_p^*}$ (Scheme 3). We hypothesize that this species is non-emissive. This assumption is based on the behaviour that we and others have found for related hydroxyphenylazoles. The experiments showed that these molecules experience a viscosity-dependent radiationless deactivation most probably associated with a large-amplitude conformational change.[28-36, 41-43, 46-52] This change is likely to be connected with a charge migration in the phototautomer originated by the previous excited-state intramolecular proton transfer, leading to a non-emissive charge-transfer species.[31-36, 47-50] Quantum mechanical calculations on several related molecules have shown that the excited tautomer possesses minimum energy at a twisted (and pyramidalized in many cases) geometry, its conformational relaxation and subsequent ultrafast internal conversion being responsible for the fast decay of the phototautomer.[30-34, 36, 46-48, 50-52] A S_0/S_1 conical intersection at the twisted geometry of the tautomer was found in some cases,[30, 36, 46, 52] but not in others.[50] According to these results, we hypothesize for **1-NMe** that after ESIPT a charge-transfer process from the phenoxy ring to the protonated imidazopyridine moiety occurs (Scheme 3), leading to a twisted (and probably pyramidalized) TICT structure of biradicaloid nature, $\mathbf{T_p^*(CT)}$**,** responsible for the ultrafast radiationless deactivation of **1-NMe**.

Under the above hypothesis, the weak fluorescence detected for **1-NMe** in trifluoroethanol solution must be due to the existence in this solvent of detectable amounts of ground-state conformers of $\mathbf{N_p}$ which lack the intramolecular hydrogen bond ($\mathbf{N_{p\text{-}open}}$, Scheme 3), thus preventing the occurrence of the ESIPT-TICT process and allowing fluorescence to compete successfully. The high hydrogen-bond donor ability α of trifluoroethanol (see Table 3) would facilitate the formation of a strong hydrogen bond of the solvent with imidazole nitrogens, breaking the intramolecular hydrogen bond of **1-NMe**. We must suppose nevertheless that the $\mathbf{N_{p\text{-}open}}$ conformers would also exist in water or other alcohols, as they have strong hydrogen-bond acceptor ability β in addition to fairly high α values, thus facilitating the formation of several intermolecular hydrogen bonds of the solute with the hydroxylic solvent molecules (see Scheme 3). Taking into account that water and ethanol have a higher capacity to accept a proton from the solute than trifluoroethanol, we interpret the lack of fluorescence for **1-NMe** open conformers in these solvents as being due to its dissociation taking place in the excited state, affording the

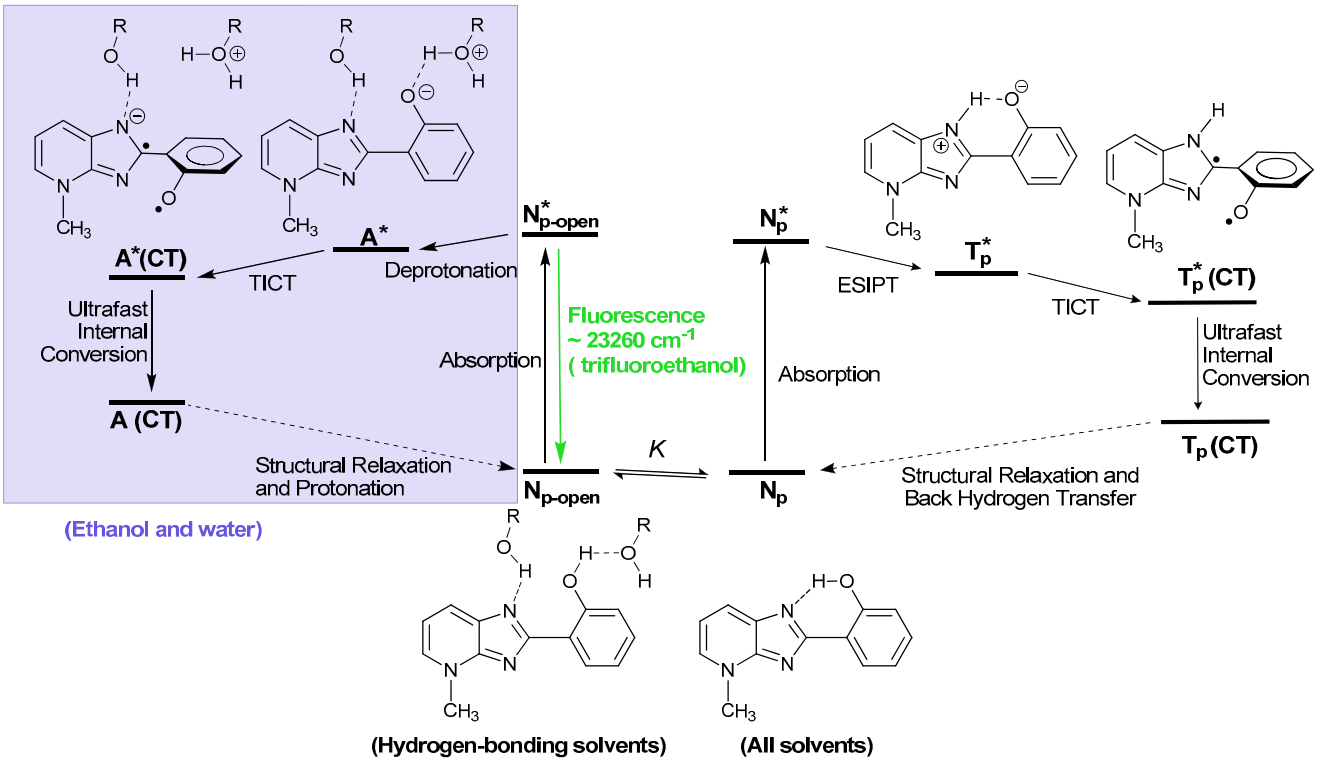

Scheme 3 Excitation and deactivation pattern proposed for **1-NMe** in neutral media.

excited anion **A*** in water and ethanol. As we have shown (Table 3), the **1-NMe** anion is non-fluorescent, probably also due to a TICT process affording the charge transfer state **A*(CT)**, facilitated by the negative charge on the electron donor moiety (see Scheme 3). Similar excited-state dissociation of the open conformers of ESIPT dyes in hydrogen-bonding solvents has been found in many cases,[28, 45, 65, 76, 79] causing in TICT-prone molecules an increase in the radiationless deactivation.[28]

4.5 Excited-state behaviour of 1-NMe in acidic solutions: ESIPT and Photodissociation

1-NMe exhibited quite intense fluorescence emission in acidified acetonitrile and trifluoroethanol, which overlapped the absorption band (see Fig. 4 and Table 1). The excitation and emission spectra were independent of the monitoring wavenumber and the fluorescence decay was monoexponential in acetonitrile at any wavenumber (Table 2), indicating that a unique species is responsible for the fluorescence emission. Nevertheless, in addition to the ground-state precursor of the only fluorescent species, at least another non-fluorescent cation must be present in acidified acetonitrile and trifluoroethanol solutions, as the fluorescence excitation spectrum did not match the absorption spectrum (Fig. 4).

Fig. 9 illustrates the possible configurations of protonated **1-NMe**. Two non-equivalent imidazole positions are available for the proton (1*H* and 3*H*), and each isomer may have the hydroxyl group in *syn* or *anti* position with respect to the pyridine nitrogen. From the four resulting isomers, two may form an intramolecular hydrogen bond N···H–O, and the other two an N–H···OH bond. We may suppose that the isomers with intramolecular hydrogen bond N···H–O probably experience an ultrafast ESIPT from the hydroxyl group to the nitrogen upon excitation ($\mathbf{C_p1}H^*_{syn}$ and $\mathbf{C_p3}H^*_{anti}$ would originate the tautomeric cations $\mathbf{TC}^*_{syn}$ and $\mathbf{TC}^*_{anti}$). Based on the behaviour discussed above in section 4.4 for neutral **1-NMe**, we hypothesize that the high positive charge on the imidazopyridine ring of the tautomeric cations triggers a charge-transfer process from the phenoxy ring to the protonated imidazopyridine ring, this process leading to a non-emissive twisted structure ($\mathbf{TC}^*_{\mathbf{anti}}\mathbf{(CT)}$ in Scheme 4). We may assume therefore that $\mathbf{TC}^*_{syn}$ and $\mathbf{TC}^*_{anti}$ are non-fluorescent species, and that one or both of its precursors $\mathbf{C_p1}H^*_{syn}$ and $\mathbf{C_p3}H^*_{anti}$ would be responsible for the absorption bands of **1-NMe** in acidified acetonitrile and trifluoroethanol solutions that do not produce detectable fluorescence emission (see Fig. 4). The absence of a large Stokes-shifted band in the fluorescence spectrum of cationic **1-NMe** supports this interpretation, as this type of band is characteristic of the emission of molecules after ESIPT.

On the basis of the previous analysis, one of the species $\mathbf{C_p3}H^*_{syn}$ or $\mathbf{C_p1}H^*_{anti}$, with intramolecular hydrogen bond N–H···OH and precluded ESIPT, must be responsible for the fluorescent emission of protonated **1-NMe** in acetonitrile and trifluoroethanol. The monoexponential decays monitored at several emission wavenumbers indicate that probably one of them is in much greater concentration than the other, but the fluorescence measurements do not allow a more concrete assignment.

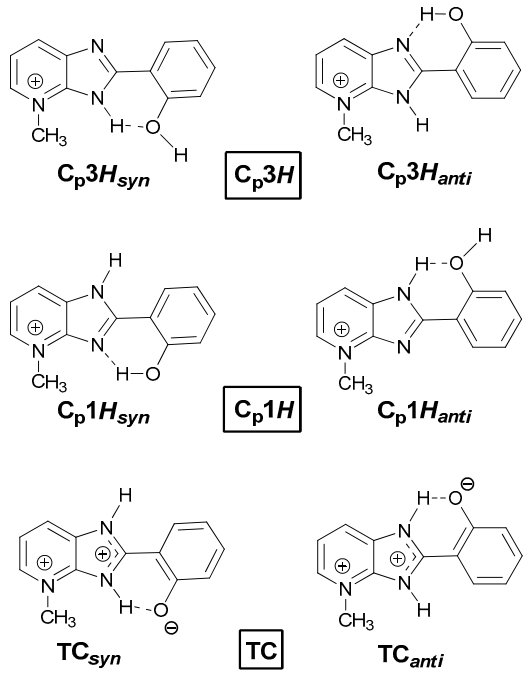

Fig. 9 Molecular structures of several isomers of **1-NMe** cation. Hydrogen-bonded conformers and tautomers of the pyridinium cation ($\mathbf{C_p}$) and tautomeric cation (**TC**) obtained after ESIPT are shown. 1*H* and 3*H* indicate the site of the imidazole hydrogen, whilst *syn* and *anti* indicate the relative positions of the oxygen atom and the pyridine nitrogen.

By contrast with the behaviour in acetonitrile and trifluoroethanol, no fluorescence could be detected for **1-NMe** in acidified ethanol and water with 25% EtOH. In these solvents, the tautomeric cations **TC***, probably formed by ESIPT in $\mathbf{C_p1}\boldsymbol{H^*_{syn}}$ or $\mathbf{C_p3}\boldsymbol{H^*_{anti}}$ as in acetonitrile and trifluoroethanol, would be likewise non-emissive. The different behaviour must come then from the lack of emission of $\mathbf{C_p3}\boldsymbol{H^*_{syn}}$/$\mathbf{C_p1}\boldsymbol{H^*_{anti}}$ in ethanol and water. It is unlikely that this fact is due to these species being in very low concentration in the ground state in ethanol and water, as it is well known from related systems that the high hydrogen-bond ability of these solvents favour the species with the weaker intramolecular hydrogen bond N–H···OH, $\mathbf{C_p3}\boldsymbol{H_{syn}}$ and $\mathbf{C_p1}\boldsymbol{H_{anti}}$.[65, 76, 85] Comparison of the properties of the solvents studied led us to conclude that the negligible basicity of acetonitrile and trifluoroethanol is most likely the common characteristics of these solvents affecting the fluorescence properties of **1-NMe**, as the polarity is similar for acetonitrile and the alcohols, and the capacity to donate a hydrogen bond is similar for trifluoroethanol and water. The striking difference in the fluorescence behaviour of **1-NMe** in acetonitrile/trifluoroethanol and ethanol/water is then probably due to the capacity of the last solvents to act as bases, accepting a proton from the solute. This capacity must be related to the known increase in acidity of the hydroxyl group upon excitation, especially for protonated derivatives of aromatic alcohols. The cations of several molecules structurally related to **1-NMe** behave as very strong photoacids in proton-accepting solvents, yielding the neutral tautomer.[65, 76, 80, 85-87] We hypothesize that protonated **1-NMe** experiences also a fast dissociation in the excited state, generating the neutral tautomer $\mathbf{T^*_p}$ (Scheme 4). As we stated in the previous section, this species probably has a negligible fluorescence.

Our global interpretation of the fluorescence behaviour of protonated **1-NMe** is summarized in Scheme 4. A ground-state equilibrium between isomers with intramolecular hydrogen bond N···H–O and N–H···OH exist (to simplify the figure, we have depicted in Scheme 4 only the species $\mathbf{C_p1}\boldsymbol{H_{anti}}$ and $\mathbf{C_p3}\boldsymbol{H_{anti}}$, but similar behaviour is expected for the species $\mathbf{C_p3}\boldsymbol{H_{syn}}$ and $\mathbf{C_p1}\boldsymbol{H_{syn}}$; we don't have information about the main isomers present in solution). The molecules with N···H–O intramolecular hydrogen bond undergo an ESIPT-TICT process upon excitation, which results in a fast radiationless deactivation. The molecules with N–H···OH intramolecular hydrogen bond and precluded ESIPT would either deactivate and emit fluorescence, or rapidly dissociate in proton-accepting solvents. The dissociated species would originate a non-emissive TICT state.

Conclusions

We have synthesized the novel ESIPT dye **1-NMe**, whose fluorescence is undetectable in neutral media, except in hydrogen-bonding and very weakly basic solvents like trifluoroethanol, where it shows a feeble fluorescence. This fact indicates a very efficient radiationless deactivation of the first-excited singlet state. Based on the behaviour of similar molecules, we propose that upon excitation, **1-NMe** experiences an ultrafast ESIPT process to form a proton-transferred tautomeric species, which would undergo a TICT process and consequent very fast radiationless deactivation. The fraction of ground-state tautomers intermolecularly hydrogen bonded to the solvent would deprotonate and experience afterwards also a TICT process and fast radiationless deactivation. The exception would be trifluoroethanol, due to the inability of this solvent to accept the photodissociated proton, which allows observing the fluorescence of the small fraction of open tautomers in this solvent. The very efficient excited-state deactivation of **1-NMe** suggests that this kind of structure could be useful as a new family of UV photoprotectors.

We have found that protonation of **1-NMe** takes place at one of the benzimidazole nitrogens. The cation shows intense fluorescence in acetonitrile and trifluoroethanol, but is non-emissive in ethanol and water. We interpret these facts as being due to the photoacid properties of **1-NMe** cation and the different basicities of these solvents. The tautomers of cationic **1-NMe** with a N–H···OH intramolecular hydrogen bond would behave as strong photoacids, rapidly dissociating at the hydroxyl group in solvents like water and ethanol and giving rise to the non-fluorescent neutral species. On the contrary, the same tautomers would decay by fluorescence emission and radiationless deactivation in solvents like acetonitrile and trifluoroethanol, unable to accept the proton. Moreover, the absence of fluorescence from a proton-transferred form for cationic **1-NMe** indicates that the tautomers with intramolecular hydrogen bond N···H–O most

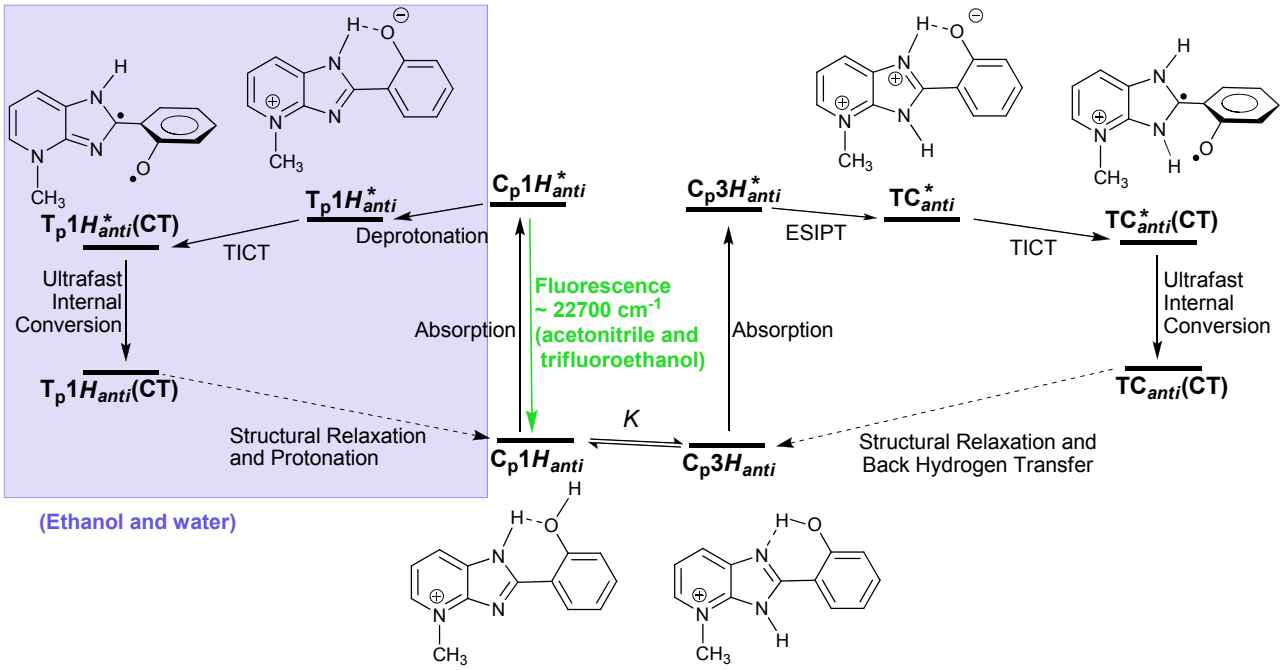

Scheme 4 Excitation and deactivation pattern proposed for **1-NMe** in acidic solutions. A similar mechanism is expected for the ground-state species $\mathbf{C_p3}H_{syn}$ / $\mathbf{C_p1}H_{syn}$

probably experience an ESIPT-TICT process, causing a very fast radiationless deactivation of those conformers in all the solvents examined.

Excitation of neutral **1-OMe** in acetonitrile, ethanol, and water lead to its own emission. However, a large fraction of **1-OMe** molecules gets protonated at the pyridine nitrogen in trifluoroethanol, which proves its strong photobasic properties.

Protonation of **1-OMe** takes place at the imidazole and pyridine nitrogens. The presence of the two cations in the ground state was detected in all of the solvents studied, the pyridinium cation being always the main component. The amount of the imidazolium cation is increased when the hydrogen-bond donor ability of the solvent increases. The absorption and fluorescence spectra of the two cations are strongly overlapped. We devised a method to resolve the overlapping spectra by applying a principal component global analysis to a series of excitation spectra taken at different monitoring emission wavenumbers. In the analysis, we assumed that the coefficients presented a log-normal dependence with the external parameter (monitoring emission wavenumbers). This procedure allowed us to resolve the components of the absorption and fluorescence spectra of cationic **1-OMe** and estimate the equilibrium constant between the cations in several solvents. The method developed could be useful for other cases of overlapping structureless spectra of fluorescent species in equilibrium.

Acknowledgements

We are indebted to the Spanish Ministry of Education and Science and the European Regional Development Fund (Grants CTQ2007-68057-C02-01/BQU and CTQ2010-17835) and the Xunta de Galicia (Grant IN845B-2010/094) for financial support of our work. A. Brenlla thanks the Fundación Segundo Gil Dávila for a postgraduate research grant.

Notes and references

[a] *Departamento de Química Física e Centro Singular de Investigación en Química Biolóxica e Materiais Moleculares, Universidade de Santiago de Compostela, E-15782 Santiago de Compostela, Spain. E-mail: carmen.rios@usc.es, manuel.mosquera@usc.es, flor.rodriguez.prieto@usc.es.*

1 S. J. Formosinho and L. G. Arnaut, *J. Photochem. Photobiol. A*, 1993, **75**, 21-48.

2 S. M. Ormson and R. G. Brown, *Prog. React. Kinet.*, 1994, **19**, 45-91.

3 T. Elsaesser and H. J. Bakker, *Ultrafast Hydrogen Bonding Dynamics and Proton Transfer Processes in the Condensed Phase*, Kluwer Acad. Pub., Dordrecht, 2002.

4 J. T. Hynes, J. T. Klinman, H. H. Limbach and R. L. Schowen, *Hydrogen-Transfer Reactions*, Wiley-VCH, Weinheim, 2007.

5 K.-L. Han and G.-J. Zhao eds., *Hydrogen Bonding and Transfer in the Excited State*, Wiley, Chichester, 2010.

6 N. Mataga, H. Chosrowjan and S. Taniguchi, *J. Photochem. Photobiol. C*, 2005, **6**, 37-79.

7 Z. R. Grabowski, K. Rotkiewicz and W. Rettig, *Chem. Rev.*, 2003, **103**, 3899-4031.

8 V. Volchkov and B. Uzhinov, *High Energy Chem.*, 2008, **42**, 153-169.

9 S. Scheiner, *J. Phys. Chem. A*, 2000, **104**, 5898-5909.

10 C. H. Kim and T. Joo, *Phys. Chem. Chem. Phys.*, 2009, **11**, 10266-10269.

11 F. Y. Dupradeau, D. A. Case, C. Z. Yu, R. Jimenez and F. E. Romesberg, *J. Am. Chem. Soc.*, 2005, **127**, 15612-15617.

12 Q. Chu, D. A. Medvetz and Y. Pang, *Chem. Mat.*, 2007, **19**, 6421-6429.

13 A. P. deSilva, H. Q. N. Gunaratne, T. Gunnlaugsson, A. J. M. Huxley, C. P. McCoy, J. T. Rademacher and T. E. Rice, *Chem. Rev.*, 1997, **97**, 1515-1566.

14 J. F. Callan, A. P. de Silva and D. C. Magri, *Tetrahedron*, 2005, **61**, 8551-8588.

15 B. Valeur and I. Leray, *Coord. Chem. Rev.*, 2000, **205**, 3-40.

16 S. Park, S. Kim, J. Seo and S. Y. Park, *Macromol. Res.*, 2008, **16**, 385-395.

17 S. Park, J. E. Kwon, S. H. Kim, J. Seo, K. Chung, S. Y. Park, D. J. Jang, B. M. Medina and J. Gierschner, *J. Am. Chem. Soc.*, 2009, **131**, 14043-14049.

18 K. Jayaramulu, P. Kanoo, S. J. George and T. K. Maji, *Chem. Commun.*, 2010, **46**, 7906-7908.

19 C. C. Hsieh, C. M. Jiang and P. T. Chou, *Acc. Chem. Res.*, 2010, **43**, 1364-1374.

20 C. C. Hsieh, M. L. Ho and P. T. Chou, in *Advanced Fluorescence Reporters in Chemistry and Biology I: Fundamentals and Molecular Design*, ed. A. P. Demchenko, Springer-Verlag, Berlin, 2010, pp. 225-266.

21 D. Gormin and M. Kasha, *Chem. Phys. Lett.*, 1988, **153**, 574-576.

22 A. Sytnik, D. Gormin and M. Kasha, *Proc. Natl. Acad. Sci. U. S. A.*, 1994, **91**, 11968-11972.

23 S. M. Ormson, R. G. Brown, F. Vollmer and W. Rettig, *J. Photochem. Photobiol. A*, 1994, **81**, 65-72.

24 P. T. Chou, M. L. Martinez and J. H. Clements, *J. Phys. Chem.*, 1993, **97**, 2618-2622.

25 C. C. Hsieh, Y. M. Cheng, C. J. Hsu, K. Y. Chen and P. T. Chou, *J. Phys. Chem. A*, 2008, **112**, 8323-8332.

26 J. Seo, S. Kim and S. Y. Park, *J. Am. Chem. Soc.*, 2004, **126**, 11154-11155.

27 C. H. Kim, J. Park, J. Seo, S. Y. Park and T. Joo, *J. Phys. Chem. A*, 2010, **114**, 5618-5629.

28 A. Maliakal, G. Lem, N. J. Turro, R. Ravichandran, J. C. Suhadolnik, A. D. DeBellis, M. G. Wood and J. Lau, *J. Phys. Chem. A*, 2002, **106**, 7680-7689.

29 J. C. Suhadolnik, A. D. DeBellis, C. Hendricks-Guy, R. Iyengar and M. G. Wood, *J. Coat. Technol.*, 2002, **74**, 55-61.

30 M. J. Paterson, M. A. Robb, L. Blancafort and A. D. DeBellis, *J. Am. Chem. Soc.*, 2004, **126**, 2912-2922.

31 C. A. S. Potter, R. G. Brown, F. Vollmer and W. Rettig, *J. Chem. Soc., Faraday Trans.*, 1994, **90**, 59-67.

32 F. Vollmer and W. Rettig, *J. Photochem. Photobiol. A*, 1996, **95**, 143-155.

33 D. LeGourriérec, V. Kharlanov, R. G. Brown and W. Rettig, *J. Photochem. Photobiol. A*, 1998, **117**, 209-216.

34 S. Kim, J. Seo and S. Y. Park, *J. Photochem. Photobiol. A*, 2007, **191**, 19-24.

35 S. Ríos Vázquez, M. C. Ríos Rodríguez, M. Mosquera and F. Rodríguez-Prieto, *J. Phys. Chem. A*, 2007, **111**, 1814-1826.

36 H.-H. G. Tsai, H.-L. S. Sun and C.-J. Tan, *J. Phys. Chem. A*, 2010, **114**, 4065-4079.

37 M. H. V. Huynh and T. J. Meyer, *Chem. Rev.*, 2007, **107**, 5004-5064.

38 S. Hammes-Schiffer and A. V. Soudackov, *J. Phys. Chem. B*, 2008, **112**, 14108-14123.

39 N. A. Shaath, *Photochem. Photobiol. Sci.*, 2010, **9**, 464-469.

40 A. P. Fluegge, F. Waiblinger, M. Stein, J. Keck, H. E. A. Kramer, P. Fischer, M. G. Wood, A. D. DeBellis, R. Ravichandran and D. Leppard, *J. Phys. Chem. A*, 2007, **111**, 9733-9744.

41 P. F. Barbara, L. E. Brus and P. M. Rentzepis, *J. Am. Chem. Soc.*, 1980, **102**, 5631-5635.

42 W. Al-Soufi, K. H. Grellmann and B. Nickel, *Chem. Phys. Lett.*, 1990, **174**, 609-616.

43 W. E. Brewer, M. L. Martinez and P. T. Chou, *J. Phys. Chem.*, 1990, **94**, 1915-1918.

44 Y. Nosenko, G. Wiosna-Salyga, M. Kunitski, I. Petkova, A. Singh, W. J. Buma, R. P. Thummel, B. Brutschy and J. Waluk, *Angew. Chem.-Int. Edit.*, 2008, **47**, 6037-6040.

45 R. S. Becker, C. Lenoble and A. Zein, *J, Phys. Chem.*, 1987, **91**, 3509-3517.

46 A. L. Sobolewski, W. Domcke and C. Hattig, *J. Phys. Chem. A*, 2006, **110**, 6301-6306.

47 D. LeGourriérec, V. A. Kharlanovb, R. G. Brown and W. Rettig, *J. Photochem. Photobiol. A*, 2000, **130**, 101-111.

48 M. I. Knyazhansky, A. V. Metelitsa, A. J. Bushkov and S. M. Aldoshin, *J. Photochem. Photobiol. A*, 1996, **97**, 121-126.

49 S. Ríos Vázquez, M. C. Ríos Rodríguez, M. Mosquera and F. Rodríguez-Prieto, *J. Phys. Chem. A*, 2008, **112**, 376-387.

50 F. A. S. Chipem and G. Krishnamoorthy, *J. Phys. Chem. A*, 2009, **113**, 12063-12070.

51 C. M. Estevez, R. D. Bach, K. C. Hass and W. F. Schneider, *J. Am. Chem. Soc.*, 1997, **119**, 5445-5446.

52 M. Barbatti, A. J. A. Aquino, H. Lischka, C. Schriever, S. Lochbrunner and E. Riedle, *Phys. Chem. Chem. Phys.*, 2009, **11**, 1406-1415.

53 A. O. Doroshenko, E. A. Posokhov, A. A. Verezubova, L. M. Ptyagina, V. T. Skripkina and V. M. Shershukov, *Photochem. Photobiol. Sci.*, 2002, **1**, 92-99.

54 N. Dash, F. A. S. Chipem, R. Swaminathan and G. Krishnamoorthy, *Chem. Phys. Lett.*, 2008, **460**, 119-124.

55 S. H. Yin, Y. F. Liu, W. Zhang, M. X. Gu and P. Song, *J. Comput. Chem.*, 2010, **31**, 2056-2062.

56 *US Pat.,* 6936618 B2, 2005.

57 W. J. Coates, B. Connolly, D. Dhanak, S. T. Flynn and A. Worby, *J. Med. Chem.*, 1993, **36**, 1387-1392.

58 V. Bavetsias, C. Sun, N. Bouloc, J. Reynisson, P. Workman, S. Linardopoulos and E. McDonald, *Bioorg. Med. Chem. Lett.*, 2007, **17**, 6567-6571.

59 S. K. Das and S. K. Dogra, *J. Chem. Soc., Perkin Trans. 2*, 1998, 2765-2771.

60 P. Barraclough, D. Firmin, R. Iyer, W. R. King, J. C. Lindon, M. S. Nobbs, S. Smith, C. J. Wharton and J. M. Williams, *J. Chem. Soc.-Perkin Trans. 2*, 1988, 1839-1846.

61 W. H. Melhuish, *J. Phys. Chem.*, 1961, **65**, 229-235.

62 G. A. Crosby and J. N. Demas, *J. Phys. Chem.*, 1971, **75**, 991-1024.

63 F. Rodríguez Prieto, M. Mosquera and M. Novo, *J. Phys. Chem.*, 1990, **94**, 8536-8542.

64 M. Novo, M. Mosquera and F. Rodriguez Prieto, *Can. J. Chem.*, 1992, **70**, 823-827.

65 M. Mosquera, J. C. Penedo, M. C. Ríos Rodríguez and F. Rodríguez-Prieto, *J. Phys. Chem.*, 1996, **100**, 5398-5407.

66 W. Al-Soufi, M. Novo and M. Mosquera, *Appl. Spectrosc.*, 2001, **55**, 630-636.
67 M. J. Kamlet, J. L. M. Abboud, M. H. Abraham and R. W. Taft, *J. Org. Chem.*, 1983, **48**, 2877-2887.
68 M. Novo, M. Mosquera and F. Rodríguez Prieto, *J. Phys. Chem.*, 1995, **99**, 14726-14732.
69 R. Yang and S. G. Schulman, *Luminescence*, 2001, **16**, 129-133.
70 E. Bardez, A. Chatelain, B. Larrey and B. Valeur, *Journal of Physical Chemistry*, 1994, **98**, 2357-2366.
71 D. B. Siano and D. E. Metzler, *Journal of Chemical Physics*, 1969, **51**, 1856-1861.
72 B. Valeur, *Molecular Fluorescence: Principles and Applications*, Wiley-VCH, Weinheim (Germany), 2002.
73 Z. R. Grabowski and A. Grabowska, *Z. Physik. Chem. Neue Folge*, 1976, **101**, 197-208.
74 A. Douhal, F. Amat-Guerri, M. P. Lillo and A. U. Acuna, *J. Photochem. Photobiol. A*, 1994, **78**, 127-138.
75 G. Krishnamoorthy and S. K. Dogra, *J. Lumines.*, 2000, **92**, 103-114.
76 M. C. Ríos Rodríguez, F. Rodríguez-Prieto and M. Mosquera, *Phys. Chem. Chem. Phys.*, 1999, **1**, 253-260.
77 J. Durmis, M. Karvaš and Z. Maňásek, *Collect. Czech. Chem. Commun.*, 1973, **38**, 224-242.
78 J. Catalán, E. Mena, F. Fabero and F. Amat-Guerri, *J. Chem. Phys.*, 1992, **96**, 2005-2016.
79 F. Rodriguez-Prieto, J. C. Penedo and M. Mosquera, *J. Chem. Soc., Faraday Trans.*, 1998, **94**, 2775-2782.
80 M. Mosquera, M. C. Ríos Rodríguez and F. Rodríguez-Prieto, *J. Phys. Chem. A*, 1997, **101**, 2766-2772.
81 J. Waluk, *Acc. Chem. Res.*, 2003, **36**, 832-838.
82 D. R. Lide, *Handbook of Chemistry and Physics*, CRC Press LLC, Boca Raton, 2004.
83 N. Agmon, *J. Phys. Chem. A*, 2005, **109**, 13-35.
84 L. M. Tolbert and K. M. Solntsev, *Acc. Chem. Res.*, 2002, **35**, 19-27.
85 A. Brenlla, F. Rodríguez-Prieto, M. Mosquera, M. A. Ríos and M. C. Ríos Rodriguez, *J. Phys. Chem. A*, 2009, **113**, 56-67.
86 J. C. Penedo, M. Mosquera and F. Rodríguez-Prieto, *J. Phys. Chem. A*, 2000, **104**, 7429-7441.
87 M. Bräuer, M. Mosquera, J. L. Pérez-Lustres and F. Rodríguez-Prieto, *J. Phys. Chem. A*, 1998, **102**, 10736-10745.

